Organic and Inorganic Modified Montmorillonite as a Scavenger of Formaldehyde in Modified Urea-Formaldehyde Composites

Marija Krstić[1], Suzana Samaržija-Jovanović[2,*], Tijana Jovanović[3], Vojislav Jovanović[2], Gordana Marković[4] and Milena Marinović-Cincović[5]

[1]*University of Novi Sad, Faculty of Technology Novi Sad, Novi Sad, Serbia*

[2]*University of Priština in Kosovska Mitrovica, Faculty of Sciences and Mathematics, Kosovska Mitrovica Serbia*

[3]*University of Niš, Faculty of Sciences and Mathematics, Niš, Serbia*

[4]*A.D. Tigar, Pirot, Serbia*

[5]*University of Belgrade, Vinča Institute of Nuclear Sciences, National Institute of the Republic of Serbia, Belgrade, Serbia*

Abstract: This research used montmorillonite (K10) modified with Hexadecyltrimethylammonium bromide (HDTMABr), and sulfuric acid (H_2SO_4). The samples are marked with MMT, OMMT for organic-modified montmorillonite, and AMMT for inorganic-modified montmorillonite. UF resin with a molar ratio FA/U = 0.8 was synthesized *in situ* with modified and unmodified MMT. X-ray diffraction analysis (XRD), Fourier transform infrared spectroscopy (FTIR), non-isothermal thermogravimetric analysis (TGA), and scanning electron microscopy (SEM) were used to characterize the MMT samples. The degree of activation was determined based on the measurement of specific surface area, which was determined by the Sears method. The sulfite method was used to determine free and released formaldehyde from synthesized urea-formaldehyde/montmorillonite (UF/MMT) composites. SEM analysis showed changes in the OMMT morphology and the formation of a hollow network, affecting the clay's absorption capacity. Measurement of the specific surface area shows that higher values were obtained for AMMT (183 m^2/g) compared to OMMT (13.5 m^2/g). Despite that, the free and released formaldehyde amount was 0.06% and 4.6% for UF/AMMT and 0.1% and 1.0% for UF/OMMT. The larger interlayer spacing and hydrophobic nature of OMMT make it an effective barrier within the UF resin matrix.

Keywords: Montmorillonite, Urea-formaldehyde resin, Activation, Hydrolytic stability, Formaldehyde, Organic modification.

1. INTRODUCTION

Urea-formaldehyde (UF) resins, produced through the condensation of urea (U) and formaldehyde (FA), are crucial adhesives in the wood industry, extensively used in products such as medium-density fiberboards (MDF), plywood panels, and other wood-based materials [1, 2]. These adhesives dominate the market due to their cost-effectiveness, rapid curing, and high reactivity, making them indispensable in industrial applications [3]. However, the widespread use of UF resins brings with it a significant challenge: the emission of FA, a recognized health hazard [4]. Formaldehyde, classified as a Group 1 carcinogen by the World Health Organization (WHO) and the International Agency for Research on Cancer (IARC) [5], poses serious risks, including respiratory problems, skin irritation, and long-term effects such as nasopharyngeal cancer. In 2023, the European Commission published a new regulation (Commission Regulation (EU) 2023/1464) according to which the concentration of released formaldehyde, from 2026, must not exceed 0.062 mg/m^3 for furniture and wooden products and 0.080 mg/m^3 for items other than furniture and products from wood [6]. The emission of FA from UF resins is primarily due to unreacted FA in the resin matrix and the hydrolysis of the resin structure under humid or acidic conditions [7]. While reducing the formaldehyde-to-urea (F/U) molar ratio in the resin formulation can lower FA emissions, this often compromises the adhesive's reactivity and, consequently, the quality of the finished wood products [8, 9].

To address this, researchers have explored alternative methods to mitigate FA emissions, with a significant focus on the use of formaldehyde scavengers, such as urea [10], silicon dioxide (SiO_2) [11], titanium dioxide (TiO_2) [12], montmorillonite (MMT) [13], or some biofillers (tannin, cellulose, starch) [14, 15]. Montmorillonite (MMT), a clay mineral with a distinctive layered structure and high cation-exchange

*Address correspondence to this author at the University of Priština in Kosovska Mitrovica, Faculty of Sciences and Mathematics, Lole Ribara 29, 38220 Kosovska Mitrovica; Tel: +381 28 425 396;
E-mail: vojani@sbb.rs; suzana.samarzija@pr.ac.rs

capacity (CEC), has emerged as a promising candidate for this purpose. Its structural unit consists of an octahedral layer of aluminum positioned between two tetrahedral layers of silicon dioxide. MMT's unique properties, such as its large specific surface area (SSA) and swelling capacity, make it an effective material for adsorption and catalytic processes [16, 17]. However, to fully harness MMT's potential as a formaldehyde scavenger, its physical and chemical properties often require modification.

Two primary methods, within chemical modification, for enhancing the properties of MMT are inorganic acid activation and organic modification. Inorganic acid activation, often referred to simply as acid activation, involves treating MMT with strong acids like sulfuric (H_2SO_4) or hydrochloric acid (HCl) to enhance its porosity, surface area, and surface acidity. This process leads to the removal of impurities, the leaching of structural cations, and an overall increase in the material's adsorptive capacity [18]. Acid activation can significantly alter the textural and chemical properties of MMT, making it more effective in capturing formaldehyde and other volatile organic compounds (VOCs). For instance, the activation of MMT with sulfuric acid has been shown to triple its SSA [19], thereby enhancing its ability to interact with and adsorb formaldehyde molecules. On the other hand, organic modification of MMT involves the intercalation of organic molecules, such as quaternary ammonium salts, into the clay's interlayer spaces [20]. This process transforms the hydrophilic nature of MMT into a more organophilic character [21], increasing its affinity for organic pollutants like formaldehyde. Organic modification not only improves the dispersion of MMT within polymer matrices but also enhances the clay's ability to interact with and immobilize formaldehyde within UF resins. This dual function of organic modification - improving both the mechanical properties of the composite and its environmental safety - makes it an attractive approach for researchers seeking to develop advanced materials [22].

Despite the potential benefits of both inorganic acid activation and organic modification, the literature lacks a comprehensive comparison of these two methods, particularly in the context of formaldehyde scavenging in UF composites. This gap in research underscores the need for studies that evaluate the relative effectiveness of these modification techniques. Understanding the strengths and limitations of each approach could lead to optimized strategies for reducing formaldehyde emissions from UF resins, thereby enhancing the safety and sustainability of wood-based products.

In this study, we aim to fill this gap by investigating the effects of both inorganic acid activation and organic modification on the structural, thermal, and adsorption properties of modified MMT. By comparing these two modification methods, we seek to determine which approach offers superior performance in terms of formaldehyde scavenging and overall enhancement of UF resin composites. The findings from this research will provide valuable insights into the development of more effective, environmentally friendly adhesives for the wood industry, contributing to the ongoing effort to reduce formaldehyde emissions and their associated health risks.

2. MATERIALS AND METHODS

2.1. Materials

Urea was pursached from Alkaloid (Skopje, North Macedonia), and formaldehyde, 35%, from Unis (Goražde, Bosnia and Herzegovina). Montmorillonite K10 (Sigma-Aldrich, Steinheim, Germany); Hexadecyltrimethylammonium bromide (Acros, New Jersey, USA).

2.2. Methods

Synthesis of AMMT - The modification was done by adding 10 g of MMT K10 in 100 ml of 0.75M H_2SO_4. The suspension was stirred on a magnetic stirrer for a 3h, at a temperature of 60 °C. Following the reaction period, the mixture was filtered and rinsed with distilled water to eliminate any remaining sulfate ions. The obtained AMMT was dried in an oven for 24h at 80 °C [23].

Synthesis of OMMT - 5 grams of NaMMT synthesized according to reference [19] were measured and dispersed in 100 cm^3 of distilled water for 24 hours. At the same time, a solution of HDTMABr (2.27 g in 75 cm^3 of distilled water) was prepared, which was slowly added from a burette dropwise into the clay suspension. The liquid was then decanted, and the clay was washed with distilled water until Br^- ions were detected [22].

Synthesis of modified urea-formaldehyde resins - The synthesis of UF composites with molar ratio of FA to U of 0.8 and with K10, AMMT, and OMMT was performed according to Jovanović *et al*. [24].

Determination of free FA - The quantification of free formaldehyde was conducted using the sulfite method [25]. In this procedure, 0.5 g of finely powdered resin was dispersed in 25 cm³ of distilled water. To this mixture, 5 drops of thymolphthalein indicator were added followed by careful titration with 0.1 M solution of sodium hydroxide to achieve neutralization. Subsequently, 15 cm³ of 0.5 M sodium sulfite was added, and the solution was stirred for a couple minutes to ensure thorough interaction. The mixture was then subjected to a slow titration with 0.1 M hydrochloric acid until the endpoint was determined. A blank solution, prepared without the resin, was also processed using the same procedure to ensure accuracy in the calculations. The percentage of free FA was then calculated based on the titration results. The percentage of free formaldehyde was determined using the following equation (Equation 1):

$$\mathrm{FA}(\%) = \frac{\mathrm{V} \cdot \mathrm{c} \cdot \mathrm{E} \cdot 100}{1000 \cdot \mathrm{a}} \quad (1)$$

V is the volume of HCl (dm^3); c is the concentration of HCl (mol/dm^3); E is the equivalent weight of FA, and a is the weight of the samples (g).

Acid hydrolysis of modified UF resin - The synthesized UF resins containing K10, AMMT, and OMMT were subjected to acid hydrolysis following the method outlined by Jovanović and co-workers [14]. The modified UF composites were first ground into fine particles, and then 0.5 g of each resin sample was placed into a beaker in which 50 cm³ of 0.1 M hydrochloric acid was added. The mixture was hydrolyzed under continuous and vigorous stirring using a magnetic stirrer at 50°C for 90 minutes. A blank sample, consisting of 0.5 g of the same resin, was extracted in 250 cm³ of water for 90 minutes at room temperature to serve as a control.

Determination of released FA - To quantify the formaldehyde released during hydrolysis, the sulfite method (previously explained), was used. After the hydrolysis process, a 50 cm³ aliquot of the suspension was immediately extracted and filtered. The filtrate was transferred to a beaker, diluted with ethyl alcohol to 100 cm³, and 5 drops of thymolphthalein were added as an indicator. The solution was carefully neutralized by titration with 0.1 M sodium hydroxide. Subsequently, 15 cm³ of 0.5 M sodium sulfite was added, and the mixture was stirred for 5 minutes. The solution was then titrated slowly with 0.1 M hydrochloric acid until the endpoint was reached. The same procedure was applied to the blank, and the result was factored into the final calculations. The percentage of released formaldehyde was calculated using the same equation as for free formaldehyde, as shown in Equation (1).

Determination of specific surface area (SSA) - The SSA was determined using the Sears method [26]. A 0.5 g sample of clay was acidified to a pH of 3–3.5 using 0.1 M HCl and then diluted with distilled water to a total volume of 50 cm³ after the addition of 10 g of NaCl. The mixture was titrated with a standard 0.1 M solution of NaOH, first to pH 4 and subsequently to pH 9. The specific surface area was then calculated using Equation (2):

$$\mathrm{SSA}\left(\mathrm{m}^2/\mathrm{g}\right) = 32\mathrm{V} - 25 \quad (2)$$

V is the volume of the standard solution required to raise the pH from 4 to 9

Determination of cation exchange capacity (CEC) - The cation exchange capacity was measured by titrating a montmorillonite suspension in water with a methylene blue (MB) solution, following the method described by Topal [27]. The CEC was calculated using Equation (3):

$$\mathrm{CEC} = \frac{\mathrm{c} \cdot \mathrm{V}}{\mathrm{m}} \quad (3)$$

c is the concentration of methylene blue solution (mol/dm^3), *V* is the volume of MB solution (dm^3), and *m* is the mass of sample (kg)

Attenuated Total Reflectance-Fourier Transform Infrared (ATR-FTIR) spectroscopy - The FTIR spectra of the samples were recorded using a Nicolet 380 FTIR spectrometer by Nicolet Corporation (USA). Measurements were taken in the wavenumber range of 4000 to 500 cm^{-1}, with a resolution of 4 cm^{-1} and 64 scans per spectrum.

Thermogravimetric study - Thermal stability was analyzed using a Setaram Setsys Evolution 1750 instrument. The samples were heated in alumina crucibles under an argon atmosphere at a flow rate of 20 cm³/min, within a temperature range of 30-800°C, and a heating rate of 10°C/min.

X-ray diffraction (XRD) - XRD measurements were carried out using a Rigaku MiniFlex600 diffractometer (Japan), equipped with an X-ray lamp operating at 40V/30mA and utilizing Cu Kα radiation (λ = nm). Diffraction data were collected over a 2θ range of 10°

to 80°, with a step size of 0.01° and a scanning speed of 10°/min. The crystallinity of the modified UF resin was determined from the XRD patterns using the peak deconvolution method with a Gaussian function, as described in Equation (4) [28]:

$$\text{Crystalinity}\,(\%) = \frac{\text{area of crystalline peaks}}{\text{area of all peaks}} \cdot 100 \quad (4)$$

Scanning Electron Microscopy - Micrographs of the pure and modified MMT were captured using a Tescan FE-SEM Mira 3 XMU scanning electron microscope at an acceleration voltage of 20 kV. Before imaging, the samples were sputter-coated with gold using a Polaron SC503 (Fisons Instruments).

3. RESULTS AND DISCUSSIONS

Table **1** shows the obtained results for SSA, CEC, and crystallinity for unmodified and modified K10.

It illustrates that organic modification of MMT results in decreased values for CEC, SSA, and crystallinity, and conversely, inorganic modification leads to an increase in these values. The SSA of unmodified montmorillonite K10, as determined by the Sears method, was found to be 131.9 m²/g. Following inorganic chemical modification, the SSA increased to 183 m²/g. This higher SSA suggests that inorganically activated K10 possesses a substantial number of silanol groups that can interact with organic molecules in aqueous environments [29]. According to Parker *et al*. [30], the elevated SSA value of K10 activated with acid could be attributed to the deprotonation of internal silanol groups by NaOH, since the smaller OH^- ion can penetrate the micropores more effectively than the larger nitrogen atom. For organically modified MMT, the reduction in SSA to 13.5 m²/g indicates that HDTMABr chains cover the clay surface.

SSA values typically correlate directly with CEC values. An increase in SSA usually results in an increase in CEC, which was also observed in our experiment. The CEC for unmodified MMT was 0.18, while for inorganically modified AMMT it increased to 0.30 mol/kg, and for organically modified OMMT it decreased to 0.02 mol/kg. Acid modification of MMT promotes the removal of octahedral ions like Mg, Fe, Al, and alkali metal oxides, along with tetrahedral ions from clay minerals, resulting from isomorphous substitution in crystal structures. This process typically enhances the specific surface area and adsorption capacity. For OMMT, on the other side, Klapyta with co-workers [31] demonstrated that values of CEC decrease with $HDTMA^+$ cation intercalation, indicating that during intercalation, some exchangeable hydrated cations remain unreplaced. HDTMABr can be intercalated between clay layers either through adsorption or by forming chemical bonds. The intercalation of HDTMABr increased the d-spaces between clay layers (explained in detail with XRD results), leading to a disordered clay structure and a reduction in crystallinity (Table **1**). Structural disruption is also evident in the SEM micrographs shown in Figure **2**.

Pure, unmodified K10 sample comprises montmorillonite clay, quartz, muscovite, feldspar, and kaolin [32]. Muscovite, a mica mineral, is the dominant phase in K10, while montmorillonite serves as the secondary phase [33]. In the XRD diffractograms (Figure **1**), the most intense peaks are observed at 2θ values of 26.60° for MMT, 26.47° for AMMT, and 26.65° for OMMT, all originating from quartz [34]. The intensity of this peak increases markedly after the organic modification of MMT, suggesting the incorporation of swelling agents between the clay layers. Based on Bragg's law, a shift in peaks from higher to lower diffraction angles indicates an increase in d-spacing. These changes in AMMT (from 26.60° in MMT to 26.47° in AMMT) could be attributed to the removal of interlayer cations (Mg^{2+} and Ca^{2+}) and partial protonation of the interlayer region, where interlayer cations are replaced by the oxonium ion H_3O^+ [35]. For OMMT, the shift from 8.90° 2θ for MMT to 8.85° 2θ for OMMT indicates that modifying MMT with HDTMABr increases the d-spacing values of unmodified MMT. This confirms that chains of the

Table 1: CEC, SSA, and Crystallinity of Pure and Modified MMT

Montmorillonite	CEC (mol/kg)	SSA (m^2/g)	Crystallinity (%)
MMT	0.18	131.9	75.95
AMTT	0.30	183	82.75
OMMT	0.02	13.5	68.49

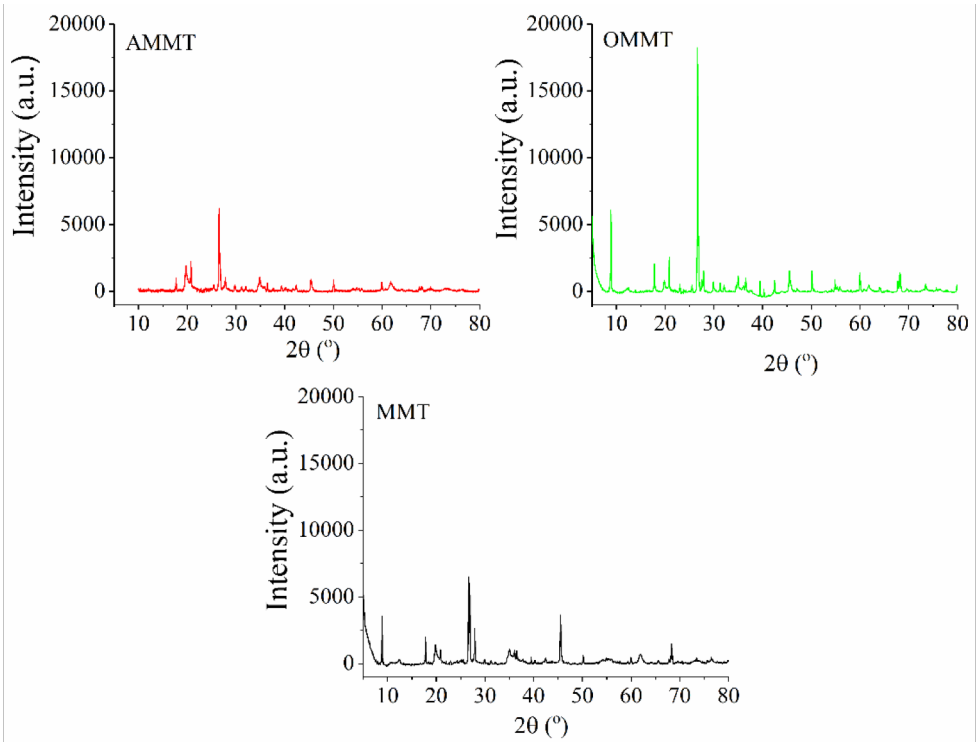

Figure 1: X-ray diffractograms of pure and modified MMT.

modifier are intercalated into the MMT layers, altering its structure. When $HDTMA^+$ cations are intercalated between MMT layers, they maximize contact with the silicate surface resulting in greater basal spacing and allowing more quaternary ammonium cations to be housed within the interlayer spaces [36].

Figure **2** presents SEM micrographs comparing the microstructure of K10 in both its modified and unmodified states.

The observed microstructures of the montmorillonite samples demonstrate variations depending on the activation method employed. As shown in Figure **2**, the acid-treated montmorillonite (Figure **2b**) largely maintained its characteristic layered structure, similar to the unmodified montmorillonite (Figure **2a**). In the case of OMMT, as seen in Figure **2c**, the grain edges exhibit twisting, resulting in the curvature of the grain edges and defoliation of aggregates, leading to the development of a network of hollows [37].

Figure **3** and Table **2** show the FTIR spectra and associated data for both unmodified and modified K10.

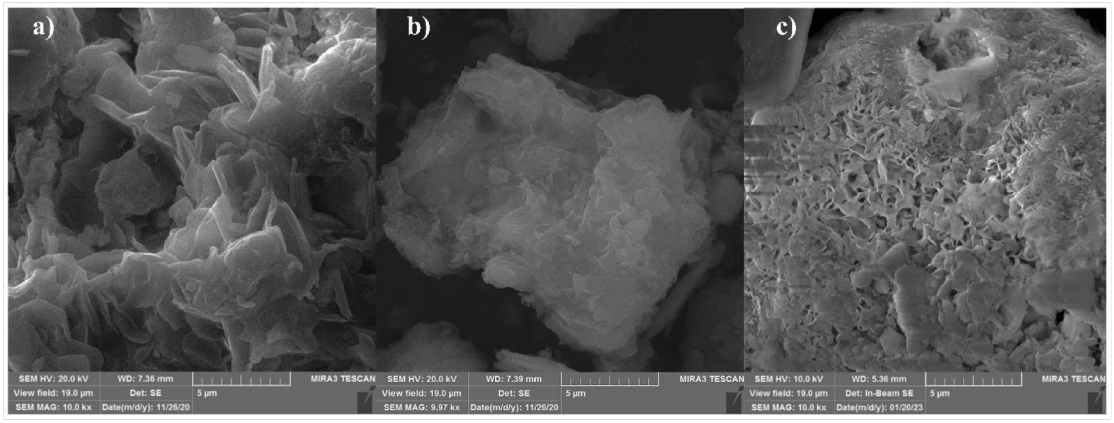

Figure 2: SEM micrographs of (**a**) pure MMT, (**b**) AMMT, and (**c**) OMMT with magnification at 10000x.

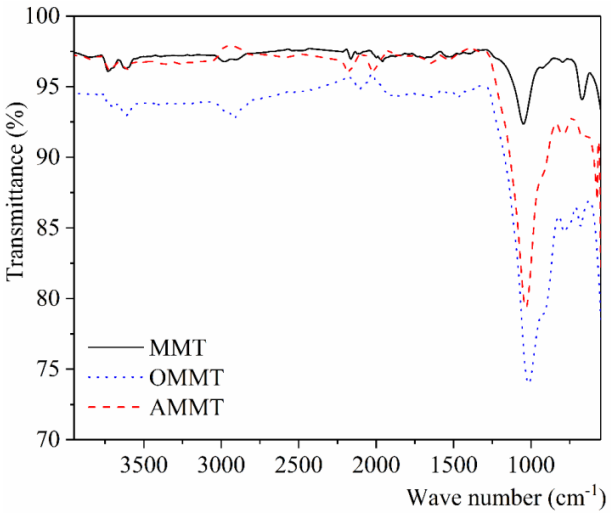

Figure 3: FTIR spectra of pure and modified MMT.

The doublet observed at approximately 3730 cm^{-1} and 3700 cm^{-1} signifies O-H stretching vibrations within Fe–OH–Al, Mg–OH–Al, and Al–OH–Al units in the octahedral layer of montmorillonite. These bands indicate coordination of the hydroxyl group with octahedral cations like Al^{3+} or Mg^{2+} [38]. The absorption bands at 2919.4 and 2854.9 cm^{-1} for OMMT result from C-H asymmetric and symmetric stretching vibrations, respectively, originating from the $–CH_2-$ group in the aliphatic organic chain surfactant, confirming the organic modification of MMT. The band at 1643 cm^{-1} is attributed to bending vibrations in the O-H plane from adsorbed water. A band near 1473 cm^{-1} in the OMMT spectra signifies bending vibrations of $–CH_2-$ from the organophilic clay, specifically from deformation vibrations of the $\delta_{as}(CH_2)$ group from $HDTMA^+$. The dominant band within the 1021 cm^{-1} - 1116 cm^{-1} range is due to Si-O valence vibrations because of silica in montmorillonite, as well as asymmetric Si-O-Si stretching. This band suggests the introduction of swelling agents in the clay post-modification. Bands around 1000 cm^{-1} and 779 cm^{-1} are linked to aluminosilicate particles. Other bands between 1100 cm^{-1} and 600 cm^{-1} are associated with the Si-O-Si group from montmorillonite. The band near 913 cm^{-1} – 927 cm^{-1} originates from Al-OH-Al vibrations. All IR spectra display characteristic vibration bands of the smectite phase, confirming its presence in all samples, consistent with XRD analysis results. A doublet at approximately 790 cm^{-1} and 750 cm^{-1} indicates the presence of quartz, while a band around 670 cm^{-1} is attributed to feldspar [39, 40].

Alterations in the surroundings of the tetrahedral Si^{4+} ion are identified by a band at 1049 cm^{-1} in MMT, which shifts to 1032 cm^{-1} in AMMT and 1116 cm^{-1} in OMMT spectra. The presence of the three bands at 2919.4 cm^{-1}, 2854.9 cm^{-1}, and 1473.4 cm^{-1} in the OMMT spectra arising from methylene group variations confirms the incorporation of $HDTMA^+$ into the clay structure, indicating successful organic modification [22].

Table 2: Characteristic IR Bands of Pure and Modified MMT, and their Possible Assignation

Pure and Modified MMT Wavenumbers (cm^{-1})			Assignment
MMT	**AMMT**	**OMMT**	
3730.3 3699.9	3717.8 3612.6	3727.7 3691.8	ν(OH) coordinated with OH cation; ν(OH) in Mg-OH-Al, Al-OH-Al, and Fe-OH-Al units in the octahedral layer in MMT
3617.8	3612	3614.6	ν(OH) in adsorbed water, and Si-OH and Al-OH of MMT
2979.4 2903.6	- -	2919.4 2854.9	ν(C-H) and ν_{ass}(C-H) in the $-CH_2-$ in the aliphatic chains of the organic surfactants; ν(CH_3-R) of the organic surfactants
1685.8	1638.4	1635.0	δ(OH) in adsorbed water, and Si-OH and Al-OH of MMT
-	-	1473.4	δ(CH_2) from the organophilic clay
1049.8	1032	1116.3	ν(Si-O) and ν_{as}(Si-O-Si) of silica in MMT
927.7	910	913.6	ν(Si-O) and ν(Al-OH-Al) bonds in MMT
795.3 751.4	790 -	786.2 749.6	ν(Si-O) of quartz; ν(Al-Si) in MMT; ν(Si-O-Fe); ν(Si-OH);
669.2	658 571	680.3	ν_{as}(Si-O-Si) of silica in MMT; δ(OH) δ(Al-O-Si) in MMT

ν-stretching vibrations, δ-bending vibration in the plane, γ-bending vibration out to the plane.

Table 3: DTG, DTA Data of Peak Values, Temperature Intervals, $T_{5\%}$, and Mass Loss from Pure and Modified MMT

Samples	Temperature Intervals (°C)	DTG peak Values (°C)	Mass Loss (%)	Total Mass Loss (%)	$T_{5\%}$ (°C)	DTA Endothermic Peak Values (°C)
MMT	30.0-177.0 380.0-600.0	80.7 475.5	5.1 4.3	9.4	52.7	87.9 173.8 610.1
AMMT	30.0-148.6 347.1-663.4	91.2 516.2	6.1 4.2	10.8	52.7	90.8
OMMT	30.0-129.0 178.0-330.0 507.0-600.0	81.3 264.6 564.9	0.7 5.0 4.5	10.3	96.5	91.3 175.5 604.1

The thermal stability of the tested samples refers to the temperature-time range in which the material can be utilized without exceeding a specified level of mass loss. The criterion for assessing thermal stability is based on the $T_{5\%}$ value, which represents the temperature at which a 5% mass loss is recorded by TGA. Table **3** presents the percentage mass loss within the temperature range for all samples, as well as DTG, DTA peak values, and $T_{5\%}$ data.

Figure **4** shows the characteristic TG and DTG curves of unmodified K10 and modified AMMT and OMMT.

Thermal analysis of both unmodified and modified montmorillonite provides valuable insights into key processes, including dehydration (occurring below 300°C), dehydroxylation (occurring between 400°C and 750°C), and the formation of thermally stable aluminosilicate minerals at temperatures exceeding 800°C [41]. Specifically, the thermal behavior of unmodified and inorganically modified K10 is characterized by two primary mass loss processes, while organically modified montmorillonite exhibits three distinct mass loss processes, as illustrated in Figure **4a**. The initial mass loss observed in unmodified K10 (5.10%) occurs within the temperature range of 30°C to 177°C, with the maximum rate of mass loss, as indicated by the DTG curve, occurring at 80.70°C. This mass loss is attributed to the evaporation of physically absorbed water and solvents present in the sample. For the modified K10, this process occurs at slightly lower temperature ranges: 30°C to 148.6°C for AMMT and 30°C to 129°C for OMMT, with DTG peaks at 91.2°C and 81.3°C, respectively. The corresponding

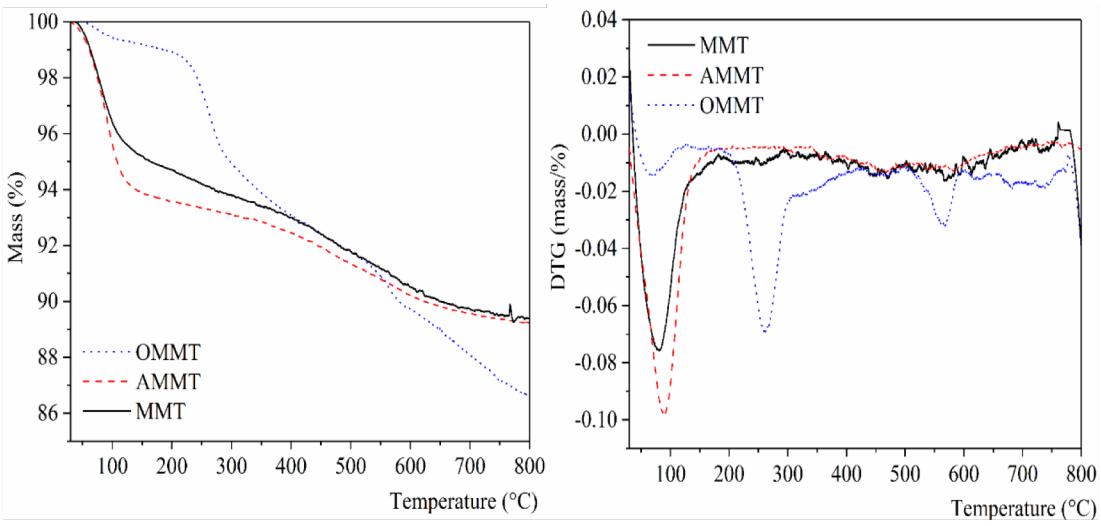

(a) (b)

Figure 4: TGA (a) and DTG (b) curves of pure and modified MMT.

mass losses for these steps are 6.1% for AMMT and 0.7% for OMMT. The DTG curves for pure MMT, AMMT, and OMMT (Figure **4b**) show a notable reduction in the amount of free and interlayer water in OMMT compared to MMT, while an increase is observed in AMMT. The reduction in free and interlayer water content in OMMT is likely due to the incorporation of HDTMABr, and due to the substitution of hydrated cations with HDTMABr, hydrophobic properties of OMMT are enhanced [22, 42]. In contrast, the acid modification of AMMT leads to an increase in specific surface area and adsorption capacity, resulting in greater absorption of free and interlayer water, and consequently, a higher percentage of mass loss during this step [39]. The second mass loss observed for pure K10 and AMMT (4.30% and 4.20%, respectively) occurs within the temperature ranges of 380–600°C for K10 and 347–663°C for AMMT, with DTG peak temperatures at 475.50°C and 468.90°C. This loss is attributed to the dehydroxylation of MMT layers. In the case of OMMT, the second mass loss (5.00%) occurs between 178°C and 330°C, with a maximum decomposition temperature of 264.60°C, primarily due to the decomposition of HDTMABr, consistent with findings reported by Naranjo *et al*. [43]. Additionally, in OMMT, a third mass loss (4.50%) is observed, which is associated with the dehydroxylation of the OMMT layers and the further decomposition of chemically adsorbed HDTMABr.

As displayed in Figure **5** and Table **3**, the DTA curves for pure K10 and OMMT display three endothermic peaks at 87.90°C, 173.80°C, and 610.10°C for MMT, and at 91.30°C, 175.50°C, and 604.10°C for OMMT.

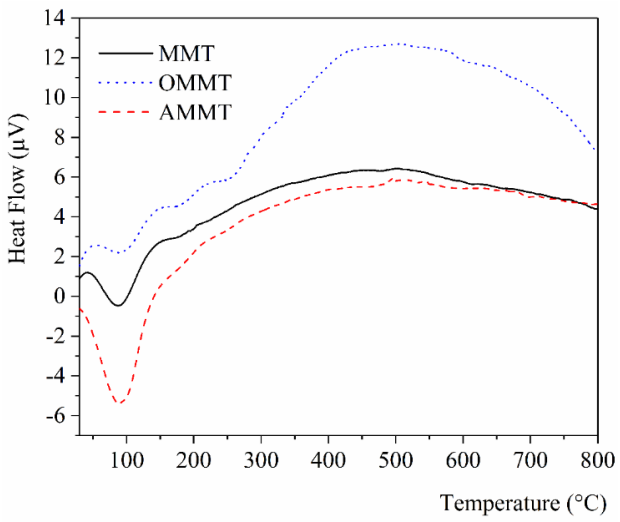

Figure 5: DTA curves of pure and modified MMT.

In contrast, the DTA curve for AMMT reveals only one endothermic peak at 90.8°C. The initial peaks are attributed to the release of adsorbed water [44]. Following modification, this peak shifts to higher temperatures, which can be explained by the increased number of O-H bonds. This increase in a number of bonds enhances the bond energy between water molecules and the surface of the MMT layers, thereby raising the dehydration temperature. The number of O-H bonds and the associated adsorption energy rise with the increase in charge density, leading to a higher dehydration temperature for montmorillonite [45]. The endothermic peaks observed at 173.8°C and 175.50°C are linked to the evaporation of exchangeable water. The smaller endothermic peaks appearing above 600°C are associated with the dehydration of silanol groups on the surface of K10 particles, resulting in a slight mass loss.

Table 3: DTG, DTA Data of Peak Values, Temperature Intervals, $T_{5\%}$, and Mass Loss from Pure and Modified MMT

Samples	Temperature Intervals (°C)	DTG Peak Values (°C)	Mass Loss (%)	Total Mass Loss (%)	$T_{5\%}$ (°C)	DTA Endothermic Peak Values (°C)
MMT	30.0-177.0 380.0-600.0	80.7 475.5	5.1 4.3	9.4	52.7	87.9 173.8 610.1
AMMT	30.0-148.6 347.1-663.4	91.2 516.2	6.1 4.2	10.8	52.7	90.8
OMMT	30.0-129.0 178.0-330.0 507.0-600.0	81.3 264.6 564.9	0.7 5.0 4.5	10.3	96.5	91.3 175.5 604.1

Thermal analysis reveals that organically modified MMT exhibits greater thermal stability compared to inorganically modified MMT and unmodified one. Considering T_5% values, which is used as thermal stability indicator, it can be concluded that OMMT exhibits greater thermal stability (96.50°C) compared to MMT K10 (52.70°C) and AMMT (52.70°C). This is evidenced by the fact that the onset of degradation for OMMT occurs at a higher temperature (Table **3**). This is likely due to the intercalation of HDTMABr, which not only increases hydrophobicity but also imparts stability under high temperatures. In contrast, the higher water content in inorganically modified MMT makes it more susceptible to thermal degradation.

Based on the results can be said that modification of montmorillonite through both inorganic and organic methods introduces significant structural and compositional changes, which in turn influence the performance of UF resins, especially in terms of formaldehyde emission. These modifications alter MMT's interaction with UF resins, affecting aspects such as adhesion, mechanical strength, and formaldehyde release. For the practical application of UF resin, one of the most important parameters to consider is the emission of formaldehyde, both free and released. Montmorillonite particles can absorb various substances due to the abundance of hydroxyl groups and oxygen atoms on their surfaces, which serve as potential active sites for formaldehyde binding. Figure **6** presents the percentages of free and released formaldehyde from UF resin with pure and activated K10 samples. The small particle size of K10 promotes their agglomeration (Figure **2a**), leading to a reduction in specific surface area and consequently diminishing the number of active sites available for FA binding. Consequently, the content of free formaldehyde-FA in the UF composites with modified K10 is lower (0.06% and 0.12%) compared to the UF composite containing unmodified K10 (0.6%). The higher CEC of inorganically modified MMT allows for better formaldehyde trapping through ion exchange mechanisms. This significantly reduces the release of formaldehyde, contributing to lower emission levels from UF resins.

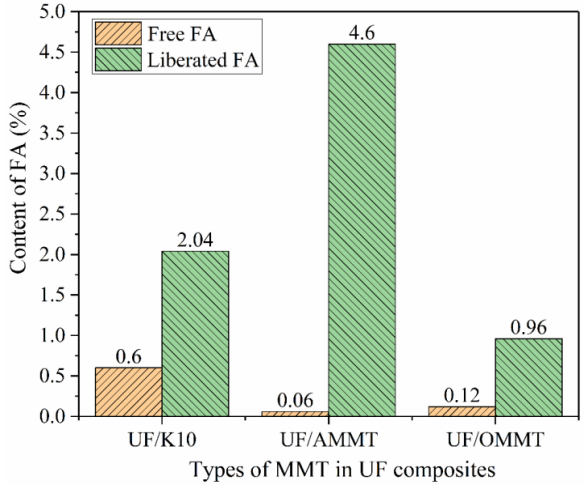

Figure 6: Percentage of free and released formaldehyde-FA from modified UF composites.

It's posited that the number of reactive groups on the surface of MMT particles is directly proportional to the specific surface area which in turn influences the material's ability to capture formaldehyde. The surface of K10 particles features silanol and non-condensed hydroxyl (-OH) groups, which are potential active sites for FA adsorption. According to Ainurofiq and co-workers [46], montmorillonite possesses Si-O/Al-O groups, O-Si-O groups, -O-Al-O groups, hydroxyl groups from water, as well as hydroxyl groups from Si-OH and Al-OH. The observed results for free formaldehyde in UF/AMMT composites align with the SSA values obtained for AMMT (Table **1**). Conversely, the results for SSA and free formaldehyde percentages in OMMT are not in correlation, possibly due to the specific surface area being determined by the Sears method rather than the Brunauer-Emmett-Teller (BET) method. The decrease in specific surface area upon modifying pure K10 indicates a reduction in the number of available silanol groups (-SiOH) on the MMT surface, which are critical for FA adsorption in aqueous media. It is also essential to consider that montmorillonite is an aluminosilicate and contains not only silanol groups but also Al-OH groups that contribute to the capture of formaldehyde [29].

The hydrolysis of UF resins is influenced by many factors, like their chemical structure or degree of cross-linking, and it can be accelerated under acidic conditions and/or elevated temperatures. This process is accompanied by the release of formaldehyde, which poses potential health risks. Formaldehyde emission occurs due to the cleavage of ether bonds and the terminal methylol groups. The hydrolysis of UF resin is considered a key factor contributing to long-term formaldehyde emissions from panels. Several studies indicate that UF resins with a lower formaldehyde-to-urea molar ratio exhibit a reduced content of terminal methylol groups and decreased structural branching [1, 47]. This reduction leads to lower adsorption of water and stronger interchain bonding. Additionally, the structure of MMT acts as a physical barrier, impeding

the diffusion of formaldehyde to the material's surface and thereby reducing formaldehyde emissions from the UF resin. The UF/AMMT composite demonstrates lower resistance to acid hydrolysis, as evidenced by a higher percentage of released FA (4.6%). In contrast, the modified UF resin containing OMMT shows the highest hydrolytic stability, with less than 1% FA released following acid hydrolysis. The larger interlayer spacing and hydrophobic nature of organically modified MMT make it an effective barrier within the resin matrix. This barrier effect can help trap formaldehyde within the resin and slow its release. Though the CEC is reduced in OMMT, the increased d-spacing and structural flexibility enable the modified clay to physically restrict formaldehyde diffusion, thus contributing to lower formaldehyde emissions.

Both inorganic and organic modifications of MMT contribute to reducing formaldehyde emission in UF resins but through different mechanisms. Inorganically modified MMT relies on its higher SSA and CEC to chemically adsorb and trap free formaldehyde. The increased interaction sites between MMT and the resin matrix enable greater adsorption of formaldehyde, leading to a more direct reduction in emissions. Organically modified MMT, on the other hand, functions by creating a physical barrier to formaldehyde diffusion. The intercalated organic chains and increased d-spacing prevent formaldehyde molecules from easily escaping the resin matrix, thus reducing emissions indirectly. In summary, both inorganic and organic modifications of montmorillonite offer significant benefits for improving the performance of UF resins, particularly by reducing formaldehyde emissions. The choice of modification method depends on the desired balance between mechanical properties, thermal stability, dispersion, and formaldehyde emission control, making each type of modified MMT suited for specific applications in UF resin formulations.

4. CONCLUSIONS

In this work, we successfully activated montmorillonite K10 using inorganic (AMMT) and organic (OMMT) chemical modification. The successful modification of montmorillonite MMT was validated through FTIR and XRD analyses, which provided clear evidence of the structural and compositional changes resulting from both inorganic and organic treatments. A detailed characterization of the unmodified and modified montmorillonite demonstrated enhanced thermal stability and significant alterations in morphology, structure, and surface properties. These changes are crucial, as they directly influence the material's performance in various applications. Upon incorporating both pure and modified montmorillonite into urea-formaldehyde resins, the modified MMT exhibited a remarkable ability to act as a formaldehyde scavenger. Quantitative analysis revealed a substantial reduction in the percentage of free FA in the modified urea-formaldehyde composites, with the UF/AMMT showing a reduction to 0.06% and UF/OMMT to 0.12%, compared to 0.6% in the unmodified UF/MMT composite. This significant decrease underscores the enhanced efficiency of modified MMT in capturing and immobilizing formaldehyde. Hydrolytic stability tests revealed that the stability of these composites follows a specific trend: UF/OMMT>UF/MMT>UF/AMMT. This order highlights the superior performance of organically modified MMT in enhancing the hydrolytic stability of UF resins. The exceptional performance of OMMT not only improves the resin's durability but also offers an environmentally sustainable solution by reducing formaldehyde emissions. This makes the organic chemical modification of MMT an attractive way to improve the overall quality and safety of UF resins.

ACKNOWLEDGMENTS

The research was funded by the Ministry of Science, Technological Development and Innovation of the Republic of Serbia (contract number 451-03-65/2024-03/200123, 451-03-66/2024-03/200017, 451-03-66/2024-03/200124 and 451-03-66/2024-03/200134), and Faculty of Sciences and Mathematics, University of Priština in Kosovska Mitrovica, Serbia (contract number IJ-2301).

CONFLICT OF INTEREST

Declare none.

REFERENCES

[1] Park BD, Causin V. Crystallinity and domain size of cured urea–formaldehyde resin adhesives with different formaldehyde/urea mole ratios. Eur Polym J. 2013; 49: 532-7. https://doi.org/10.1016/j.eurpolymj.2012.10.029

[2] Park BD, Jeong HW. Hydrolytic stability and crystallinity of cured urea–formaldehyde resin adhesives with different formaldehyde/urea mole ratios. Int. J. Adhes Adhes 2011; 31(6): 524-9. https://doi.org/10.1016/j.ijadhadh.2011.05.001

[3] Valyova M, Ivanova Y, Koynov D. Investigation of free formaldehyde quantity in the production of plywood with modified urea-formaldehyde resin. Wood, Design & Technology 2017; 6(1): 72-77, ISSN: 1857 - 8381

[4] Nuryawan A, Risnasari I, Sucipto T, Heri Iswanto A, Rosmala Dewi R. Urea-formaldehyde resins: Production, application,

and testing. IOP Conf. Ser.: Mater Sci Eng 2017; 223:012053. https://doi.org/10.1088/1757-899X/223/1/012053

[5] IARC: Formaldehyde, 2-butoxyethanol and 1-tertbutoxypropan-2-ol. IARC Monographs on the Evaluation of Carcinogenic Risks to Humans 2004; 88: 1-478

[6] Commission Regulation (EU) 2023/1464 of 14 July 2023 amending Annex XVII to Regulation (EC) No 1907/2006 of the European Parliament and of the Council as regards formaldehyde and formaldehyde releasers

[7] Lubis MAR, Park BD, Lee SM, Modification of urea-formaldehyde resin adhesives with blocked isocyanates using sodium bisulfate. Int J Adhes Adhes 2017; 73: 118-124. https://doi.org/10.1016/j.ijadhadh.2016.12.001

[8] Conner AH. Urea-Formaldehyde Adhesive Resins. In: Salamone JC. editor. Polymeric Materials Encyclopedia. New York, USA: 1996.

[9] Park BD, Kang EC, Park YJ. Effects of formaldehyde to urea mole ratio on thermal curing behavior of urea-formaldehyde resin and properties of particle board. J Appl Polym Sci 2006; 101:1787-92. https://doi.org/10.1002/app.23538

[10] Costa N, Pereira J, Martins D, Martins J, Ferra J, Cruz P, Magalhães F, Mendes A, Carvalho L. Innovative catalysts for urea-formaldehyde resins. In Minimizing the environmental impact of the forest products industries. Caldeira F., Ed.; University Fernando Pessoa, Porto. 2011.

[11] Lei H, Du G, Pizzi A, Celzard A. Influence of nanoclay on urea-formaldehyde resins for wood adhesives and its model. J Appl Polym Sci 2008; 109:2442-51. https://doi.org/10.1002/app.28359

[12] Park HS, Lee H. A novel manufacturing method of urea-formaldehyde resin with the titanium dioxide for reducing formaldehyde emission. Korean Journal of Agricultural Science 2009; 36.1: 11-18.

[13] Kostić M, Samaržija-Jovanović S, Ristić M, Jovanović T, Jovanović V, Marković G, Marinović Cincović M. Effect of montmorillonite activation method on formaldehyde content in urea-formaldehyde composites. Int J Adhes Adhes 2023; 103390. https://doi.org/10.1016/j.ijadhadh.2023.103390

[14] Jovanović V, Samaržija-Jovanović S, Petković B, Milićević Z, Marković G, Marinović-Cincović M. Biocomposites based on cellulose and starch modified urea-formaldehyde resin: Hydrolytic, thermal, and radiation stability. Polym Compos 2019; 40:1287-94. https://doi.org/10.1002/pc.24849

[15] Ristić M, Samaržija-Jovanović S, Jovanović V, Kostić M, Erceg T, Jovanović T, Marković M, Marinović-Cincović M. Hydrolytic and thermal stability of urea-formaldehyde resins based on tannin and betaine bio-fillers, J Vinyl Addit Techn 2023; 29(6): 1082-92. https://doi.org/10.1002/vnl.22024

[16] El Achaby M, Ennajih H, Arrakhiz FZ, El Kadib A, Bouhfid R, Essassi E, Qaiss A. Modification of montmorillonite by novel geminal benzimidazolium surfactant and its use for the preparation of polymer organoclay nanocomposites. Compos Part B Eng 2013; 51:310-17. https://doi.org/10.1016/j.compositesb.2013.03.009

[17] Zuoa Q, Gaoa X, Yanga J, Zhanga P, Chena G, Li Y, Shi K, Wua W. Investigation on the thermal activation of montmorillonite and its application for the removal of U(VI) in aqueous solution. J TAIWAN Inst Chem E 2017; 80: 754-776. https://doi.org/10.1016/j.jtice.2017.09.016

[18] Amari A, Gannouni H, Khan MI, Almesfer MK, Elkhaleefa AM, Gannouni A, Effect of structure and chemical activation on the adsorption properties of green clay minerals for the removal of cationic dye. Appl Sci 2018; 8: 2302-32. https://doi.org/10.3390/app8112302

[19] Stoiljković S, Todorović B. Adsorption-desorption and usable properties of bentonite-based materials. Monografy (in serbian lanque), Leskovac, 2018

[20] Jankovič L`, Madejová J, Komadel P, Jochec-Mošková D, Chodák I, Characterization of systematically selected organo-montmorillonites for polymer nanocomposites, Appl. Clay Sci 2011; 51: 438-444. https://doi.org/10.1016/j.clay.2011.01.006

[21] He H, Zhou Q, Martens WN, Kloprogge TJ, Yuan P, Xi Y, Zhu JI, Frost RL. Microstructure of $HDTMA^+$-modified montmorillonite and its influence on sorption characteristics. Clays Clay Miner 2006; 54(6): 689-696. https://doi.org/10.1346/CCMN.2006.0540604

[22] Ristić M, Samaržija-Jovanović S, Jovanović T, Jovanović V, Kostić M, Marković G, Marinović-Cincović M. Organically modified montmorillonite as an environmental adsorbent of pollutants: Formaldehyde from urea-formaldehyde resin and acid red 183 dye from the aqueous solution. J Environ Chem Eng 2024; 12(1): 111828. https://doi.org/10.1016/j.jece.2023.111828

[23] Ajemba RO. Kinetics and equilibrium modeling of lead(II) and chromium(III) ions' adsorption onto clay from Kono-bowe, Nigeria. Turkish J Eng Environ Sci 2014; 38: 455-79. https://doi.org/10.3906/muh-1402-3

[24] Jovanović V, Samaržija-Jovanović S, Petković B, Dekić V, Marković G, Marinović-Cincović M. Effect of γ-irradiation on the hydrolytic and thermal stability of micro- and nano-TiO_2 based urea-formaldehyde composites. RSC Adv 2015; 5: 59715-22. https://doi.org/10.1039/C5RA10627C

[25] Walker JF. Formaldehyde. American Chemical Society Monograph Series, 3rd edn. No. 159, New York: Reinhold Publ. Corp. 1969.

[26] Sears GW. Determination of specific surface area of colloidal silica by titration with sodium hydroxide. Anal Chem 1956; 28(12): 1981-83. https://doi.org/10.1021/ac60120a048

[27] Topal T. The use of methylene blue adsorption test to assess the clay content of the Cappadocian tuff. In: Proceedings of the 8th international congress on the deterioration and conservation of Stone, Berlin, 1996: 791-99

[28] Wibowo E, Park BD. Determination of crystallinity of thermosetting urea-formaldehyde resins using deconvolution method. Macromol Res 2020; 28: 615-24. https://doi.org/10.1007/s13233-020-8076-2

[29] Yuan L, Chen L, Chen X, Liu R, Ge G. In situ measurement of surface functional groups on silica nanoparticles using solvent relaxation nuclear magnetic resonance. Langmuir 2017; 33(35): 8724-29. https://doi.org/10.1021/acs.langmuir.7b00923

[30] Parker SF, Klehm U, Albers PV. Differences in morphology and vibrational dynamics of crystalline, vitreous and amorphous silica - commercial implications. Mater Adv 2020; 1: 749-59. https://doi.org/10.1039/D0MA00158A

[31] Klapyta Z, Fujita T, Iyi N. Adsorption of dodecyl- and octadecyltrimethylammonium ions on a smectite and synthetic micas. Appl Clay Sci 2001; 19: 5-10. https://doi.org/10.1016/S0169-1317(01)00059-X

[32] Kakasaheb YN, Prashant SN, Vijay VB. Synthesis of oxygenated fuel additives via acetylation of bio-glycerol over H_2SO_4 modified montmorillonite K10 catalyst. Progress Petrochem Sci 2018; 1(1): PPS.000501. https://doi.org/10.31031/PPS.2018.01.000501

[33] Jiang JQ, Zeng Z. Comparison of modified montmorillonite adsorbents Part II: The e□ects of the type of raw clays and modification conditions on the adsorption performance.

Chemosphere 2003; 53: 53-62.
https://doi.org/10.1016/S0045-6535(03)00449-1

[34] Marsh A, Heath A, Patureau P, Evernden M, Walker P, Alkali activation behaviour of un-calcined montmorillonite and illite clay minerals. Appl Clay Sci 2018; 166: 250-261.
https://doi.org/10.1016/j.clay.2018.09.011

[35] Krupskaya VV, Zakusin SV, Tyupina EA, Dorzhieva OV, Zhukhlistov AP, Belousov PE, Timofeeva MN. Experimental study of montmorillonite structure and transformation of its properties under treatment with inorganic acid solutions. Minerals 2017; 7: 49-64.
https://doi.org/10.3390/min7040049

[36] Xu SH, Sheng GY, Boyd SA. Use of organoclays in pollution abatement, Adv Agron 1997; 59: 25-62

[37] Marras SI, Tsimpliaraki A, Zuburtikudis I, Panayiotou C. Thermal and colloidal behavior of amine-treated clays: The role of amphiphilic organic cation concentration. J Colloid Interf Sci 2007; 315: 520-527.
https://doi.org/10.1016/j.jcis.2007.06.023

[38] Ahmed A, Chaker Y, Belarbi EH, Abbas O, Chotard JN, Abassi HB, Nguyen Van Nhien A, El Hadri M, Bresson S. XRD and ATR/FTIR investigations of various montmorillonite clays modified by monocationic and dicationic imidazolium ionic liquids. J Mol Struct 2018; 1173: 653-64.
https://doi.org/10.1016/j.molstruc.2018.07.039

[39] Samaržija-Jovanović S, Jovanović V, Jovanović T, Petković B, Marković G, Porobić S, Marinović-Cincović M. Synthesis, characterization, hydrolytic, and thermal stability of urea–formaldehyde composites based on modified montmorillonite K10. Journal of Thermal Analysis and Calorimetry 2022; 147(9).
https://doi.org/10.1007/s10973-022-11238-2

[40] Madejova J, Palkova H, Pentrak M, Komadel P Near-infrared spectroscopic analysis of acid-treated organo-clays. Clay Clay Miner 2009; 57: 392-403.
https://doi.org/10.1346/CCMN.2009.0570311

[41] Živica V, Palou MT. Physico-chemical characterization of thermally treated bentonite. Compos Part B Eng 2015; 68: 436-45
https://doi.org/10.1016/j.compositesb.2014.07.019

[42] He H, Ding Z, Zhu J, Yuan P, Xi Y, Yang D, Frost RL. Thermal Characterization of Surfactant-Modified Montmorillonites, Clay Clay Miner 2005; 53: 287-293.
https://doi.org/10.1346/CCMN.2005.0530308

[43] Naranjo PM, Sham EL, Castellon ER, Torres Sanchez RM, Farfan Torres EM. Identification and quantification of the interaction mechanisms between the cationic surfactant HDTMA-BR and montmorillonite. Clay Clay Miner 2013; 61(2): 98-106.
https://doi.org/10.1346/CCMN.2013.0610208

[44] Samaržija-Jovanović S, Jovanović V, Konstantinović S, Marković G, Marinović-Cincović M. Thermal behavior of modified urea-formaldehyde resins. J Therm Anal Calorim. 2011; 104: 1159-66.
https://doi.org/10.1007/s10973-010-1143-8

[45] Tiwari RR, Khilar KC, Natarajan U. Synthesis and characterization of novel organo-montmorillonites. Appl Clay Sci 2008; 38: 203-8.
https://doi.org/10.1016/j.clay.2007.05.008

[46] Ainurofiq A, Nurcahyo I, Yulianto R. Preparation, characterization and formulation of nanocomposite matrix Na-montmorillonite intercalated medium molecular weight chitosan for theophylline sustained release tablet, Int J Pharm Pharm Sci 2014; 6(1): 131-37

[47] Dazmiri MK, Kiamahalleh MV, Dorieh A, Pizzi A. Effect of the initial F/U molar ratio in urea-formaldehyde resins synthesis and its influence on the performance of medium density fiberboard bonded with them. Int J Adhesion Adhes 2019; 95: 102440.
https://doi.org/10.1016/j.ijadhadh.2019.102440

Received on 24-08-2024 Accepted on 16-09-2024 Published on 24-09-2024

https://doi.org/10.31875/2410-4701.2024.11.06